SEMARAK ILMU PUBLISHING

Journal of Advanced Research in Applied Sciences and Engineering Technology

Journal homepage: https://semarakilmu.com.my/journals/index.php/applied_sciences_eng_tech/index
ISSN: 2462-1943

Efficient Integration of PV Panels and Electrolysis through a High-Performance Converter for Clean Hydrogen Generation

Omar Abdel-Rahim[1,2*], Al Amir Hassan[2], Ayman A. Arafa[2]

[1] Department of Electrical Engineering, Aswan University, 81542 Aswan, Egypt
[2] Department of Electrical Engineering, Egypt-Japan University of Science and Technology, Alexandria, Egypt
[3] Department of Mathematics, Faculty of Science, Sohag University, 82524, Sohag, Egypt

ARTICLE INFO

Article history:
Received 21 December 2023
Received in revised form 14 August 2024
Accepted 18 August 2024
Available online 20 September 2024

Keywords:
Green power generation; renewable energy sources; step-down isolated dc-dc converter; photovoltaic panels

ABSTRACT

Green power generation revolves around producing clean hydrogen. This is achieved through a process of generating hydrogen by electrolysis, which draws power from renewable energy sources. In this manuscript, a high performance step-down isolated dc-dc converter is proposed to interface the Photovoltaic (PV) panels and the electrolysis. This converter is highly efficient and capable of toggling on and off with minimal power consumption. The primary function of the electrolyser is to generate hydrogen, and the quantity of hydrogen produced correlates with the amount of electricity (current) it receives. To ensure seamless operation, a control system is employed. This system monitors the current and voltage of the electrolyser, ensuring it remains within optimal levels. To assess the efficacy of the proposed configuration, the system is simulated in MATLAB platform and a complete hardware in the loop test is performed using OPAL-RT OP4510.

1. Introduction

Hydrogen is a versatile energy carrier that can be produced from various sources and used for various applications. One of the potential uses of hydrogen is power generation, which can offer high energy efficiency, environmental and social benefits, and economic competitiveness. Hydrogen can be burned in a fuel cell or an internal combustion engine, creating only water as a by-product. Hydrogen power generation has the potential to reduce carbon emissions from traditional power generation assets and to support the integration of renewable power sources [1-7].

According to the International Energy Agency (IEA), the worldwide generation of hydrogen was approximately 74 million tonnes in 2019. The majority of this hydrogen was produced using fossil fuels, primarily natural gas, which accounted for around 76% of total hydrogen production. The remaining 24% was produced using low-carbon or zero-carbon methods, such as electrolysis of water using renewable electricity or nuclear power. The IEA's Sustainable Development Scenario (SDS) envisions a significant increase in the use of low-carbon hydrogen, reaching approximately 530

* *Corresponding author.*
E-mail address: o.abdelrahim@aswu.edu.eg

https://doi.org/10.37934/araset.52.2.2634

million tonnes per year by 2050. This would require a rapid expansion of low-carbon hydrogen production capacity, as well as significant investment in infrastructure and technology, see Figure 1(a) [8].

One of the most common methods for producing hydrogen is electrolysis, which uses an electric current to split water molecules into hydrogen and oxygen. Electrolysis can be powered by renewable energy sources such as solar and wind, making it a clean and sustainable way to produce hydrogen. However, the efficiency of electrolysis is limited by the power electronics used to control the electric current [9].

The over-voltage caused by concentration is not significant if the current density during operation is below 1 A/cm2. On the other hand, the concentration over potential would only be noticeable at "very high current densities" and would not be a problem in PEM water electrolysers used in commercial applications. Figure 1(b) shows the simulated cell voltage for a proton exchange membrane electrolyser [10-12].

The usual range for current density in commercial PEM electrolysers is 0.6-2.0 A/cm2. Figure 1 indicates that the concentration overvoltage plays a more significant role in PEM water electrolysis, but it can be disregarded in alkaline electrolysis since the current density is generally less than 0.5 A/cm2 [13].

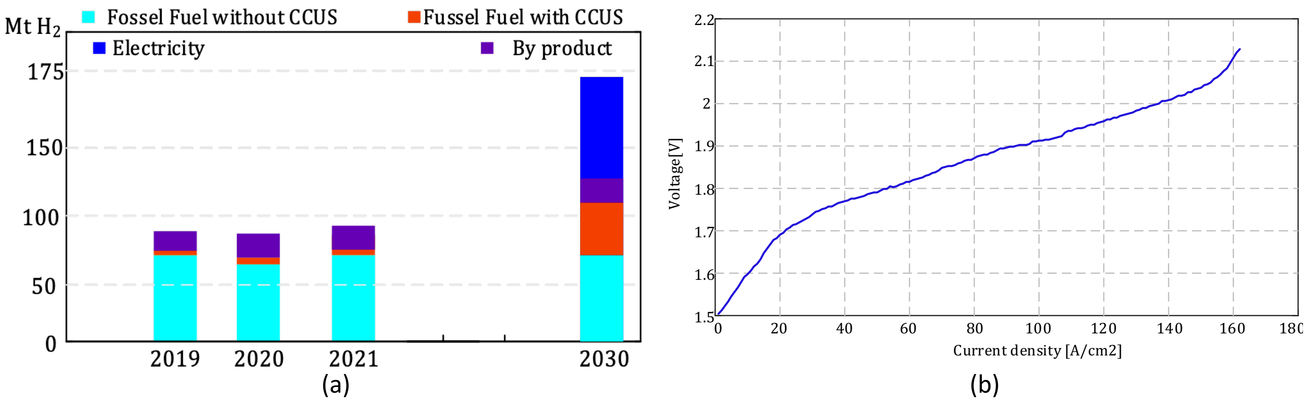

Fig. 1. (a) Global hydrogen production by technology in the net zero scenario, 2019-2030 (b) Relation between voltage level and current concentration in hydrogen electrolyser

The system design depicted in Figure 2 showcases the arrangement. Photovoltaic (PV) panels are linked to the step-down isolated direct current to direct current (dc-dc) converter's input, while the output side is connected to the electrolyzing cells. The proposed dc-dc converter adopts the push-pull full bridge configuration. Notably, this converter is capable of facilitating soft switching, specifically zero voltage/current switching. This characteristic holds considerable appeal as it minimizes losses within the system, thereby enhancing converter efficiency.

The control system is responsible for monitoring the output voltage and current. Its role is to finely adjust these parameters based on the distinct requirements of the cells. This control mechanism ensures stable operation, even when faced with fluctuations in the input side conditions.

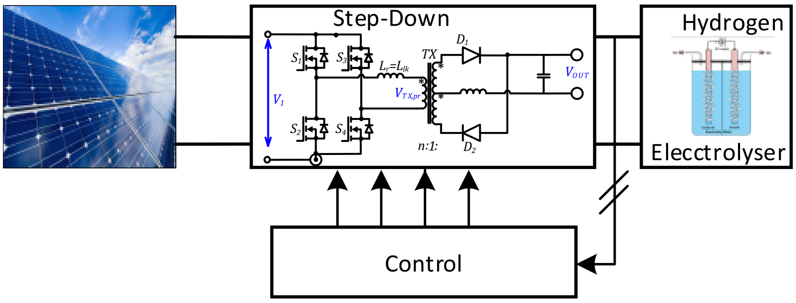

Fig. 2. Configuration of the proposed hydrogen generation system

2. Proposed Converter Operation

The proposed configuration of the converter is outlined in Figure 3. The high-voltage segment of the converter is constructed using a full-bridge inverter, a three-winding transformer, while the low-voltage side employs a push-pull setup [14-18]. To prevent transformer saturation, the full-bridge inverter cyclically alters the polarity across the transformer. Notably, this converter offers bidirectional power flow, galvanic isolation, and soft switching operation for all semiconductor components over a wide range of input power and voltage. An illustrative representation of the fundamental waveform for the proposed converter is provided in Figure 4 and possible operating modes are illustrated in Figure 5. To prevent any risk of short-circuiting the dc-source, simultaneous activation of S1 and S2, as well as S3 and S4, is prohibited. Similar restrictions apply to switches D1 and D2. The power switches within the h-bridge experience voltage stress equivalent to the input voltage, whereas switches S5 and S6 endure voltage stress akin to the converter's output voltage, as clearly outlined in Table 1.

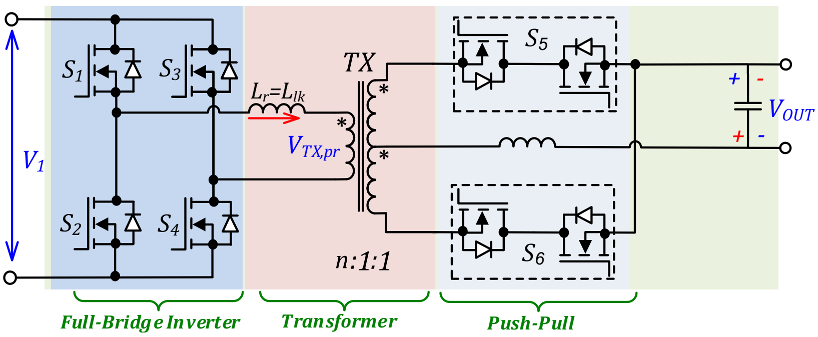

Fig. 3. Proposed bidirectional power converter

In the positive half cycle, from 0 to Ts/2, S1 and S4 are in an active state, facilitating the flow of current from the source to the transformer. Concurrently, S1 and S3 are engaged in a circulating pattern. During the subsequent negative half cycle, Ts/2 to Ts, S2 and S3 are triggered for active operation, while the freewheeling effect is realized through the activation of S2 and S4. It's important to note that diodes D1 and D2operate in a complementary fashion, ensuring smooth functioning.

To ensure the effective implementation of soft switching for all switches, the switching and resonance frequencies are aligned. The resonance frequency of the converter is defined by the following expression:

$$f_r = {}^{1}\!/_{2\pi\sqrt{L_r C_r}} \tag{1}$$

where f_r, L_r, and C_r are resonance frequency, resonance inductance and resonance capacitance, respectively. Circuit power switches voltage stress is illustrated in Table 1. H-bridge switches are under voltage stress equal to the input voltage, while push-pull switches are facing voltage stress equal to the output voltage.

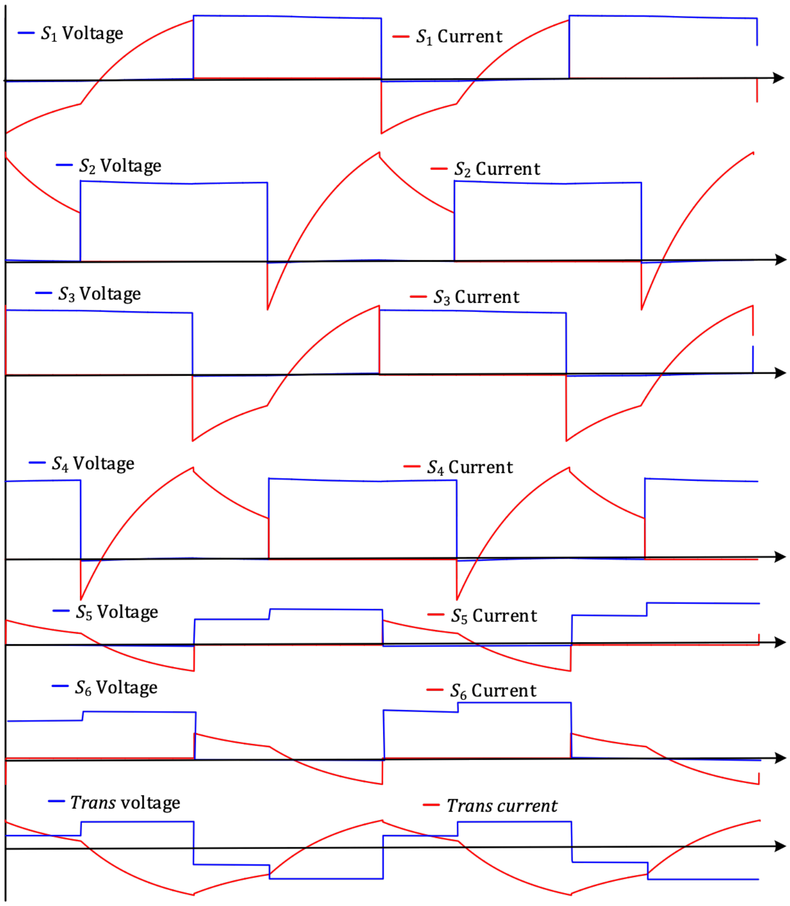

Fig. 4. Basic waveform of the proposed converter

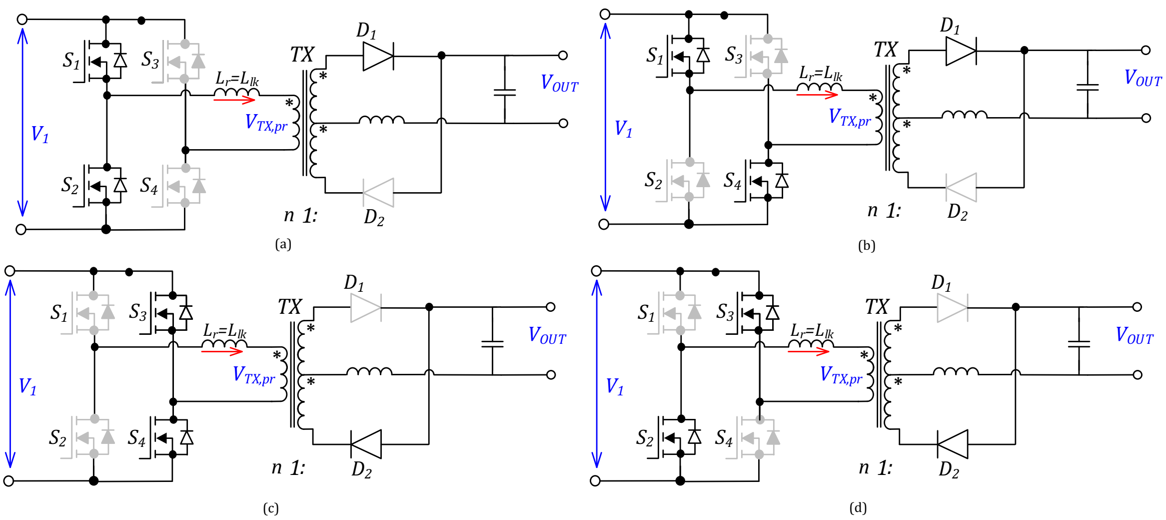

Fig. 5. Possible operating condition for the developed system

Table 1
Circuit component voltage stress

Parameter	Value
S_1	V_{in}
S_2	V_{in}
S_3	V_{in}
S_4	V_{in}
S_5	V_{co}
S_6	V_{co}

Here, the resonance frequency (f_r), resonance inductance (L_r), and resonance capacitance (C_r) contribute to the resonant behavior of the system.

The voltage stress on the circuit's power switches is outlined in Table 1. Within the H-bridge arrangement, the switches experience voltage stress at the level of the input voltage. Conversely, for the push-pull configuration, the switches contend with voltage stress equivalent to the output voltage.

3. Control System Operation

An electrolyser is a current-driven device, and the volume of produced hydrogen is proportional to the applied current density [19]. Electrolyzers operate at a fixed stack current, and the electrolyzer stack accepts DC power input from its onboard power converter [20-22]. Therefore, it can be concluded that a fixed current is required to operate the hydrogen electrolyzer. While voltage is important in the electrolysis process, it is not a constant factor. Typically, 1.5 volts are required to split water molecules into their constituent oxygen and hydrogen atoms. However, the voltage required for electrolysis can vary depending on factors such as the type of electrolyte used and the temperature of the electrolyte.

The control system for the developed system is designed to fix the output current across the electrolyser, A Proportional Integral (PI) controller is selected to control the phase-shift of the developed converter to supply the required currents to the cells

The optimal PI controller in the continuous-time domain for a single-input single-output (SISO) system is represented in the Laplace domain as [23-25]:

$$U = G_C(S)E(S) \tag{2}$$

$$G_C(S) = K_C(1 + \frac{1}{T_i S}) \tag{3}$$

Using K_C as the proportional gain, and T_i as the integral time constant, if Ti is set to infinity (resulting in P control), it becomes evident that the measured value y in the closed-loop system will consistently remain lower than the desired value r, see Figure 6. This holds true for processes lacking an integrator term, where a positive error is necessary to maintain the measured value stably and keep it lower than the desired value.

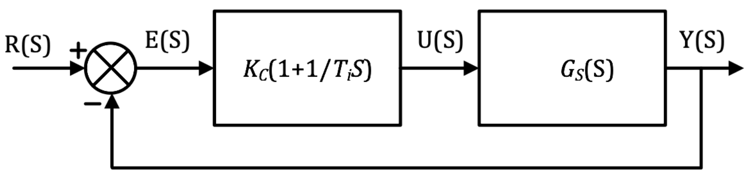

Fig. 6. Illustrates the configuration of the control system

Incorporating integral action facilitates achieving equilibrium between the measured value and the desired value. This is achieved by generating an escalating controller output in response to a constant error.

4. Simulation and Discussion

To ensure the effective functionality of the developed system, a validation process is undertaken through the creation of a simulation model within the MATLAB Simulink platform. The simulation incorporates the distinctive attributes of the PV array and the hydrogen electrolyser, as delineated in Tables 2 and 3, respectively. This meticulous validation procedure seeks to confirm the accurate and reliable performance of the system by embracing a virtual environment that mirrors the real-world conditions. Through this simulation framework, the intricate interplay between the PV array and the hydrogen electrolyser is assessed, providing a comprehensive analysis of their collective behavior.

Table 2
PV array electrical characteristics

Electrical Characteristics	
Maximum Power (W)	213W
Cells per module (Ncell)	60
Open circuit voltage Voc (V)	36.3
Short-circuit current Isc (A)	7.84
Voltage at maximum power point Vmp (V)	29
Current at maximum power point Imp (A)	7.35
Temperature coefficient of Voc (%/deg.C)	-0.36099
Temperature coefficient of Isc (%/deg.C)	0.102

Table 3
Hydrogen electrolyser characteristics

Electrical Characteristic	Value
Rated input voltage(V)	380
Operating voltage range(V)	320 - 400
Rated input current(A)	50
Electrolysis efficiency (%)	80
Nominal power consumption(W)	19,000
Output hydrogen production rate (Nm³/h)	10
Cell voltage(V)	1.8
Cell current(A)	25
Faraday efficiency (%)	95
Stack temperature(°C)	60
Cooling system power(W)	500

The PV array's power-voltage (P-V) curve, showcasing its response to alterations in radiation at the instant of 0.25 seconds, is depicted in Figure 7. This alteration in radiation gives rise to the emergence of two distinct peaks in the curve, measuring 200 W and 420 W respectively.

The converter employed in this system is not configured to maximize power extraction from the PV array. Instead, its design purpose is centered around providing a consistent current input to the hydrogen electrolyser cells. Consequently, the emphasis here lies in achieving precise current control. The observed data, as presented in Figure 8, encompasses measurements of PV voltage, current, and power. These measurements depict the adaptability of the PV array's current and voltage to cater to load requirements amidst fluctuations in radiation input.

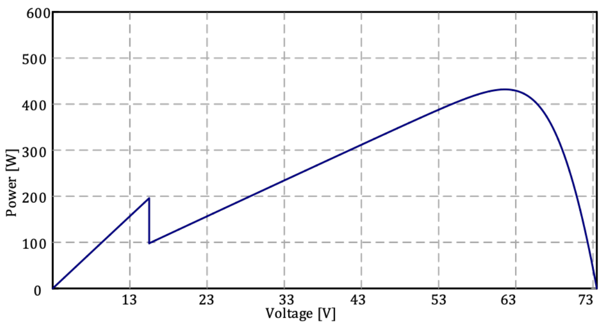

Fig. 7. P-V curve of simulated PV-array

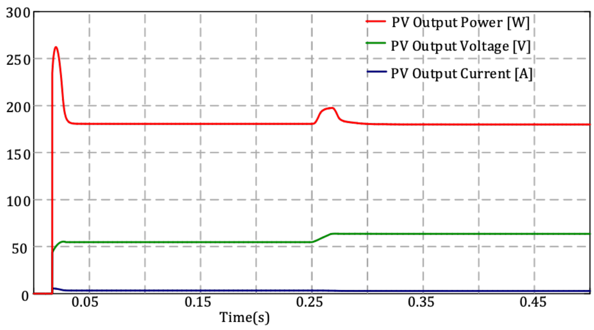

Fig. 8. Voltage, current, and power of the simulated PV array

Further insights into the system's behavior can be gleaned from Figure 9, wherein both PV array voltage and hydrogen electrolyser voltage trends are charted. Notably, while PV voltage experiences variations, the voltage across the electrolyser remains steady and unchanged.

Examining Figure 10, the electrolyser's current and the PV array's current are laid out. Even in the face of a sudden and pronounced change in radiation occurring at 0.25 seconds, the output current remains consistently maintained at the designated voltage level.

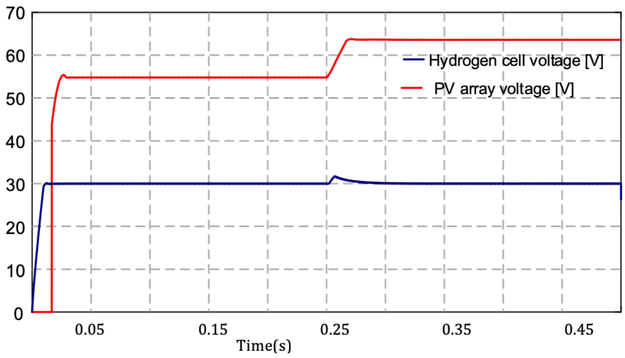

Fig. 9. PV and hydrogen electrolyser voltage

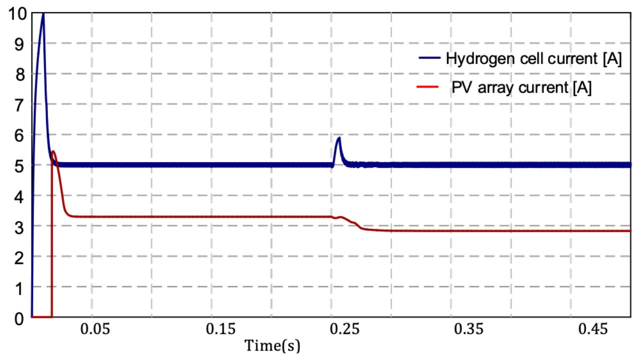

Fig. 10. PV and hydrogen electrolyser currents

The system's practical implementation is evaluated through hardware-in-the-loop testing, employing the OPAL-RT OP4510 platform. The interrelationships between input currents, output currents, input voltages, and output voltages are vividly depicted in Figure 11 for currents and Figure 12 for voltages, elucidating the comprehensive understanding of the system's dynamic behavior.

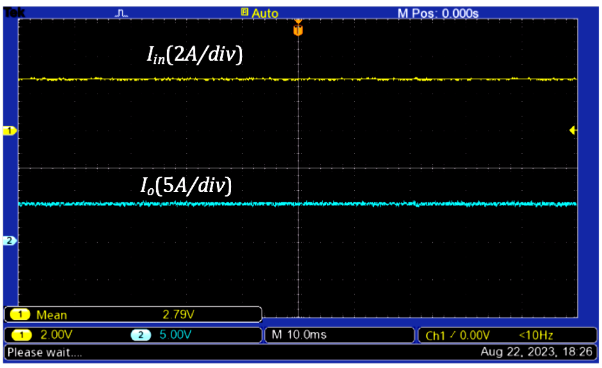

Fig. 11. Measured input output currents

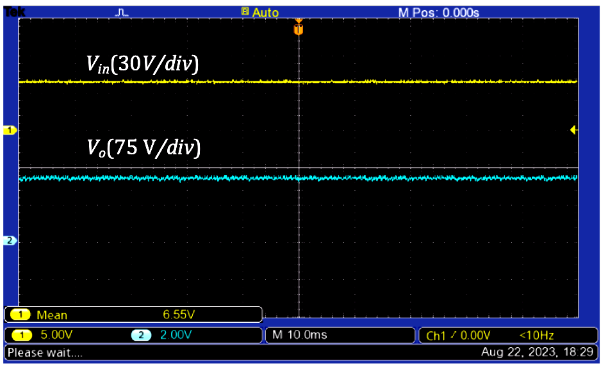

Fig. 12. Measured input and output voltage

5. Conclusion

This paper presented a push-pull buck converter for clear hydrogen generation. The converter is designed to supply the required voltage and current for the hydrogen electrolyser from PV array. Due to the nature of the Hydrogen electrolyser, the converter is controlled to inject a fixed current source to the cells away from the power fluctuations in the fuel cells. Possible operating conditions and basics waveforms are illustrated. The system is simulated in MATLAB Simulink with closed loop. The focal role of the converter within the system takes precedence. While not geared toward maximal power extraction from the PV array, its design pivot lies in delivering a stable current input to the hydrogen electrolyser cells. This precision in current control is underscored by the data presented in Figure 9, which encompasses measurements of PV voltage, current, and power. The adaptable response of the PV array to fluctuations in radiation input, in order to meet load requirements, is a testament to the system's versatility.

References

[1] Qazi, Umair Yaqub. "Future of hydrogen as an alternative fuel for next-generation industrial applications; challenges and expected opportunities." *Energies* 15, no. 13 (2022): 4741. https://doi.org/10.3390/en15134741

[2] Ahmed, Hassan Yousif, Omar Abdel-Rahim, and Ziad M. Ali. "New high-gain transformerless dc/dc boost converter system." *Electronics* 11, no. 5 (2022): 734. https://doi.org/10.3390/electronics11050734

[3] Ridhwan, Asmawi Marullah, Muhd Ridzuan Mansor, Noreffendy Tamaldin, Fahamsyah Hamdan Latief, and Viktor Vekki Ronald Repi. "Effect of KOH concentration on the performance of HHO generator at varying plate surface textures." *Journal of Advanced Research in Fluid Mechanics and Thermal Sciences* 106, no. 2 (2023): 116-128. https://doi.org/10.37934/arfmts.106.2.116128

[4] Sorrenti, Ilaria, Theis Bo Harild Rasmussen, Shi You, and Qiuwei Wu. "The role of power-to-X in hybrid renewable energy systems: A comprehensive review." *Renewable and Sustainable Energy Reviews* 165 (2022): 112380. https://doi.org/10.1016/j.rser.2022.112380

[5] Abdel-Rahim, Omar, and Haoyu Wang. "Five-level one-capacitor boost multilevel inverter." *IET Power Electronics* 13, no. 11 (2020): 2245-2251. https://doi.org/10.1049/iet-pel.2020.0033

[6] Yusof, Siti Nurul Akmal, Mat Sazilin Ayub, Saiful Bahri Mohamed, Yutaka Asako, Wan Mohd Arif Aziz Japar, Mohd Sani Said, and Mohd Shahir Kasim. "Oxyhydrogen gas production by alkaline water electrolysis and the effectiveness on the engine performance and gas emissions in an ICEs: A mini-review." *Journal of Advanced Research in Fluid Mechanics and Thermal Sciences* 97, no. 1 (2022): 168-179. https://doi.org/10.37934/arfmts.97.1.168179

[7] Bhandari, Ramchandra, and Ronak Rakesh Shah. "Hydrogen as energy carrier: Techno-economic assessment of decentralized hydrogen production in Germany." *Renewable Energy* 177 (2021): 915-931. https://doi.org/10.1016/j.renene.2021.05.149

[8] Bethoux, Olivier. "Hydrogen fuel cell road vehicles and their infrastructure: An option towards an environmentally friendly energy transition." *Energies* 13, no. 22 (2020): 6132. https://doi.org/10.3390/en13226132

[9] Orhan, Mehmet F., Ibrahim Dincer, Marc A. Rosen, and Mehmet Kanoglu. "Integrated hydrogen production options based on renewable and nuclear energy sources." *Renewable and Sustainable Energy Reviews* 16, no. 8 (2012): 6059-6082. https://doi.org/10.1016/j.rser.2012.06.008

[10] Genovese, Matteo, Alexander Schlüter, Eugenio Scionti, Francesco Piraino, Orlando Corigliano, and Petronilla Fragiacomo. "Power-to-hydrogen and hydrogen-to-X energy systems for the industry of the future in Europe." *International Journal of Hydrogen Energy* 48, no. 44 (2023): 16545-16568. https://doi.org/10.1016/j.ijhydene.2023.01.194

[11] Herlambang, Yusuf Dewantoro, Fatahul Arifin, Totok Prasetyo, and Anis Roihatin. "Numerical analysis of phenomena transport of a proton exchange membrane (PEM) fuel cell." *Journal of Advanced Research in Fluid Mechanics and Thermal Sciences* 80, no. 2 (2021): 127-135. https://doi.org/10.37934/arfmts.80.2.127135

[12] Amin, Muhammad, Hamad Hussain Shah, Bilal Bashir, Muhammad Azhar Iqbal, Umer Hameed Shah, and Muhammad Umair Ali. "Environmental assessment of hydrogen utilization in various applications and alternative renewable sources for hydrogen production: A review." *Energies* 16, no. 11 (2023): 4348. https://doi.org/10.3390/en16114348

[13] Hosseini, Seyed Ehsan, and Mazlan Abdul Wahid. "Hydrogen from solar energy, a clean energy carrier from a sustainable source of energy." *International Journal of Energy Research* 44, no. 6 (2020): 4110-4131. https://doi.org/10.1002/er.4930

[14] Abdel-Rahim, Omar, Andrii Chub, Dmitri Vinnikov, and Andrei Blinov. "DC integration of residential photovoltaic systems: A survey." *IEEE Access* 10 (2022): 66974-66991. https://doi.org/10.1109/ACCESS.2022.3185788

[15] Kanimozhi, T. "Hybrid PV and fuel cell generating system for shipboard applications based on optimal dispatch evaluator algorithm." *Journal of Advanced Research in Applied Sciences and Engineering Technology* 36, no. 2 (2023): 131-146. https://doi.org/10.37934/araset.36.2.131146

[16] Abdel-Rahim, Omar, Andrii Chub, Andrei Blinov, Dmitri Vinnikov, and Naser Hassanpour. "Step-up current-source partial power converter for PV systems." In *2022 IEEE 13th International Symposium on Power Electronics for Distributed Generation Systems (PEDG)*, pp. 1-6. IEEE, 2022. https://doi.org/10.1109/PEDG54999.2022.9923250

[17] Abdel-Rahim, Omar, Andrii Chub, Andrei Blinov, and Dmitri Vinnikov. "Current-fed dual inductor push-pull partial power converter." In *2022 IEEE 20th International Power Electronics and Motion Control Conference (PEMC)*, pp. 327-332. IEEE, 2022. https://doi.org/10.1109/PEMC51159.2022.9962937

[18] Abdel-Rahim, Omar, Andrii Chub, Andrei Blinov, and Dmitri Vinnikov. "Series buck-boost partial power converter based on the push-pull converter." In *IECON 2022–48th Annual Conference of the IEEE Industrial Electronics Society*, pp. 1-5. IEEE, 2022. https://doi.org/10.1109/IECON49645.2022.9968574

[19] Ufa, R. A., A. S. Vasilev, A. L. Gusev, A. V. Pankratov, Ya Yu Malkova, and A. S. Gusev. "Analysis of the influence of the current-voltage characteristics of the voltage rectifiers on the static characteristics of hydrogen electrolyzer load." *International Journal of Hydrogen Energy* 46, no. 68 (2021): 33670-33678. https://doi.org/10.1016/j.ijhydene.2021.07.183

[20] Abdel-Rahim, Omar, and Hirohito Funato. "A novel model predictive control for high gain switched inductor power conditioning system for photovoltaic applications." In *2014 IEEE Innovative Smart Grid Technologies-Asia (ISGT ASIA)*, pp. 170-174. IEEE, 2014. https://doi.org/10.1109/ISGT-Asia.2014.6873784

[21] Dawood, Furat, Martin Anda, and G. M. Shafiullah. "Hydrogen production for energy: An overview." *International Journal of Hydrogen Energy* 45, no. 7 (2020): 3847-3869. https://doi.org/10.1016/j.ijhydene.2019.12.059

[22] Abdel-Rahim, Omar, and Hirohito Furiato. "Switched inductor quadratic boosting ratio inverter with proportional resonant controller for grid-tie PV applications." In *IECON 2014-40th Annual Conference of the IEEE Industrial Electronics Society*, pp. 5606-5611. IEEE, 2014. https://doi.org/10.1109/IECON.2014.7049358

[23] Mohan, Ned, Tore M. Undeland, and William P. Robbins. *Power electronics: converters, applications, and design*. John wiley & sons, 2003.

[24] Ariffin, Nurul Izzah Mohamad, Nor Farahaida Abdul Rahman, and Siti Zaliha Mohammad Noor. "Hybrid one-cycle-PI control algorithm for shunt active power filter in mitigating harmonic currents." *Journal of Advanced Research in Applied Sciences and Engineering Technology* 33, no. 1 (2023): 31-43. https://doi.org/10.37934/araset.33.1.3143

[25] Kazimierczuk, Marian K., and Dariusz Czarkowski. *Resonant power converters*. John Wiley & Sons, 2012.